

Extending the LHC Reach for New Physics with Sub-Millimeter Displaced Vertices

Hayato Ito^a, Osamu Jinnouchi^b, Takeo Moroi^a, Natsumi Nagata^a, and Hidetoshi Otono^c

^a*Department of Physics, University of Tokyo, Tokyo 113-0033, Japan*

^b*Department of Physics, Tokyo Institute of Technology, Tokyo 152-8551, Japan*

^c*Research Center for Advanced Particle Physics, Kyushu University,
Fukuoka 819-0395, Japan*

Abstract

Particles with a sub-millimeter decay length appear in many models of physics beyond the Standard Model. However, their longevity has been often ignored in their LHC searches and they have been regarded as promptly-decaying particles. In this letter, we show that, by requiring displaced vertices on top of the event selection criteria used in the ordinary search strategies for promptly-decaying particles, we can considerably extend the LHC reach for particles with a decay length of $\gtrsim 100 \mu\text{m}$. We discuss a way of reconstructing sub-millimeter displaced vertices by exploiting the same technique used for the primary vertex reconstruction on the assumption that the metastable particles are always pair-produced and their decay products contain high- p_T jets. We show that, by applying a cut based on displaced vertices on top of standard kinematical cuts for the search of new particles, the LHC reach can be significantly extended if the decay length is $\gtrsim 100 \mu\text{m}$. In addition, we may measure the lifetime of the target particle through the reconstruction of displaced vertices, which plays an important role in understanding the new physics behind the metastable particles.

1 Introduction

New metastable massive particles are predicted in a variety of extensions of the Standard Model (SM) [1], and have been explored at colliders such as the LHC. If these particles have a decay length (*i.e.*, the product of the lifetime τ and the speed of light c) of $\mathcal{O}(1)$ m or shorter, then their decay can occur within tracking detectors and thus it is in principle possible to directly observe their decay points, which are away from the production point. In fact, such attempts have been made in the LHC experiments. For example, the ATLAS collaboration has searched for displaced vertices (DVs) that originate from decay of long-lived particles by investigating charged tracks with a transverse impact parameter, d_0 , of $2 \text{ mm} < |d_0| < 300 \text{ mm}$, requiring that the transverse distance between DVs and any of the primary vertices be longer than 4 mm [2]. This search is therefore sensitive to metastable particles whose decay length is $c\tau \sim \mathcal{O}(1 - 1000)$ mm. The disappearing-track searches [3] can also probe a long-lived charged particle when it decays into a neutral particle which is degenerate with the charged particle in mass [4–7]; the target of these searches is $c\tau \gtrsim 10$ cm.

On the contrary, particles with a sub-millimeter decay length have been beyond the reach of these searches. Such rather short-lived particles have been often regarded as promptly-decaying particles and probed without relying on their longevity. Exceptionally, recently, Ref. [8] considered R -parity violating supersymmetric (SUSY) model to which “ordinary” search strategies does not apply, and showed that DV-based cuts may be useful for the LHC study of such a model if the decay length of the lightest SUSY particle is longer than $\mathcal{O}(100)$ μm . From the point of view of physics beyond the SM, however, there are a variety of well-motivated new particles with $c\tau \sim$ sub-millimeter besides the above case; although LHC constraints on some of those have been already stringent even with the analysis assuming that they decay promptly, inclusion of DV-based cuts upon it significantly extends the reach of those. One of the important examples for such particles is metastable gluino in SUSY models with heavy squarks [5, 9, 10]. In particular, if the squark masses are as heavy as the PeV scale, the decay length of the gluino can be $c\tau \sim \mathcal{O}(100)$ μm (assuming that the gluino mass is around TeV) [11]. Metastable SUSY particles are also found in the gauge-mediation models [12, 13], where the decay length of the next-to-lightest SUSY particle decaying into gravitino can be order sub-millimeter, as well as in R -parity violating SUSY models [14, 15]. In addition, theories of Neutral Naturalness [16, 17], hidden-valley models [18], composite Higgs models [19], dark matter models [20], and models with sterile neutrinos [21] predict metastable particles with an $\mathcal{O}(100)$ μm decay length.

In this letter, we discuss a method of searching for metastable particles with DVs that is sensitive to $c\tau \lesssim 1$ mm as well. Here, we focus on the cases where the target metastable particles are always pair-produced, which is assured if the new particles have a conserved quantum number; for instance, in R -parity conserving SUSY models, SUSY particles, being R -parity odd, are always produced in pairs. In these cases, there are two decay points in each event, which are separated from each other by order of the decay length of these particles. We reconstruct these decay vertices in a similar manner that is used for

the primary vertex reconstruction. As shown below, using this method, we can distinguish the decay vertices if these two are separated by $\gtrsim 100 \mu\text{m}$. This method therefore enables us to search for sub-millimeter DVs. By requiring DVs in addition to the event selection criteria used in the promptly-decaying particle searches, we can go beyond the reach of these searches if the target particle has a decay length of $c\tau \gtrsim 100 \mu\text{m}$. Moreover, when they are discovered, it is also possible to measure the typical distance of the two decay points and thus to estimate the decay length of the particles, which can provide important information about the nature of the new physics behind the new particles. To be specific, in this letter, we consider metastable gluinos as an example and demonstrate that the study of sub-millimeter DVs can significantly enlarge the parameter region covered by the LHC.

The organization of this letter is as follows. We first summarize how the vertex is reconstructed in Sec. 2. In Sec. 3, we describe our method to search for DVs. Then, we apply our method to the metastable gluino search and show that the LHC reach can be extended with the study of the DVs. We also point out that it is possible to measure the decay length of the metastable particle by means of DV reconstruction. Sec. 4 is devoted to conclusions and discussion.

2 Vertex Reconstruction

First, let us briefly summarize how vertices are reconstructed at the LHC experiment. In order to make the argument clear, we use the performance of the ATLAS detector. In this letter, we concentrate on the case where a number of charged particles are emitted from vertices, which is the case when the production and the decay of metastable colored particles, like gluino, occur. Then, with the precise tracking of the charged particles by inner tracking detectors, the decay vertex of the parent particle may be reconstructed.

A similar analysis, *i.e.*, track-based reconstruction of primary vertex in proton-proton collision, has been already performed by the ATLAS [22, 23] and CMS [24] collaborations from which we can estimate the accuracy of the determination of the vertex position at the LHC. In Ref. [22], charged tracks with $p_T > 400 \text{ MeV}$ were used to reconstruct the primary vertex. In Fig. 1, we show the vertex resolutions to x - and z -directions (corresponding to the directions perpendicular and parallel to the beam axis) provided by the ATLAS collaboration [22]; the green (dot-dashed) and black (dotted) lines show the data and Monte Carlo (MC) results. Thus, if a sizable number of charged tracks are associated with the vertex, we expect that the vertex position is reconstructed with the accuracy of $\mathcal{O}(10) \mu\text{m}$. This fact indicates that, if the distance between two decay vertices is longer than $\mathcal{O}(10) \mu\text{m}$ in the pair production process of metastable particles, it may be possible to distinguish two vertices. Existence of two distinct DVs can be used to reduce SM backgrounds, as we discuss below.

In the following, we quantitatively study how well we can improve the discovery reach for the new particles with the reconstruction of DVs. For this purpose, in our MC analysis, we implement an algorithm to reconstruct DVs using charged tracks. As we mentioned,

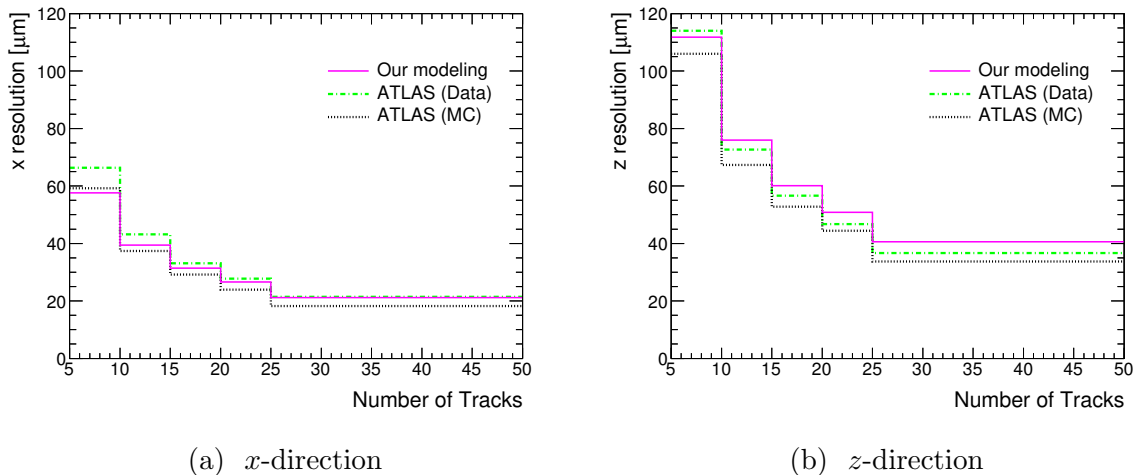


Figure 1: The resolutions of reconstructed primary vertex position as a function of the number of tracks associated with the primary vertex. The resolutions obtained with our modeling are shown in purple lines while those provided by the ATLAS collaboration [22] are shown in green dot-dashed (derived from data) and black dotted (derived from MC samples) ones.

we mainly focus on DVs which are away from the interaction point by $\lesssim 1$ mm, though our method can be used for more displaced cases as well. Our strategy to reconstruct DVs relies on tracking performance of charged-particle tracks in the inner detector.

The tracking performance of the ATLAS inner detector for $\sqrt{s} = 13$ TeV is given in Ref. [25].^{#1} To reproduce the performance of track reconstruction, we shift each track in parallel by impact parameters. We neglect the effect of the curvature of the tracks in this procedure since we focus on DVs which are very close to the interaction point. We also neglect the track parameter resolutions regarding its direction, *i.e.*, the azimuthal angle ϕ and the polar angle θ , as their resolutions are sufficiently small: $\sigma_\phi \sim 100 \mu\text{rad}$ and $\sigma_{\cot\theta} \sim 10^{-3}$ [27]. Thus, we only consider the resolutions of the transverse and longitudinal impact parameters, d_0 and $z_0 \sin\theta$, respectively. Effects of these are taken into account by random parallel shift of each track. The resolutions of the impact parameters depend on the transverse momentum p_T and the pseudorapidity η of the track. In the processes we consider in this letter, jets have relatively high p_T and do not have any preference for the small polar angle regions. In addition, it is found that the η dependences of the resolutions of the impact parameters become sufficiently small for $p_T \gtrsim$ a few GeV [27, 28]. For these reasons, we neglect the η dependences of the resolutions in this analysis. Following Ref. [27], we parametrize the p_T dependence of the track impact parameter resolutions as

$$\sigma_X(p_T) = \sigma_X(\infty) (1 \oplus p_X/p_T) , \quad (1)$$

(with $X = d_0$ and $z_0 \sin\theta$) where $\sigma_X(\infty)$ and p_X are parameters. We determine the values

^{#1}Before the LHC Run-II started, the insertable B-layer (IBL) [26] was installed, which improves the performance of track and vertex reconstruction.

of $\sigma_X(\infty)$ and p_X by fitting this expression onto the p_T dependence of the track impact parameter resolutions measured by the ATLAS collaboration [25].

Next, let us describe the procedure of the vertex reconstruction used in our analysis, which gives the best-fit point of the vertex for a given set of charged tracks. We follow the prescription given in Refs. [23]. In this prescription, the adaptive vertex fitting algorithm [29], which we briefly review in Appendix, is exploited to determine the vertex position. At the outset of this algorithm, for a given set of charged tracks, a vertex seed is found from the crossing points of the reconstructed tracks by means of a method called the fraction of sample mode with weights (FSMW) [30]. Once the initial vertex is fixed, we assign a weight, which is given in Eq. (A.3), to each track such that tracks far from the vertex point are down-weighted. We then determine another vertex position at which an objective function, which corresponds to the vertex χ^2 multiplied by the above weights, is minimized. We iterate this χ^2 fitting steps with varying a parameter for the weight assignment until the vertex position converges within $1 \mu\text{m}$. The parameters in this algorithm are set to be the default values given in Ref. [29] and references therein, though the results are rather insensitive to these parameters.

To validate our modeling of impact-parameter resolutions and the vertex reconstruction, we reconstruct the position of primary vertices in minimum-bias events using our procedure. We generate 47,000 minimum-bias event MC samples with PYTHIA v8.2 [31]. Here, we use only tracks with $p_T > 400 \text{ MeV}$ and $|\eta| < 2.5$ in accordance with the ATLAS study [22]. (For this choice of minimal p_T , the best-fit values of $\sigma_{d_0}(\infty)$ ($\sigma_{z_0 \sin \theta}(\infty)$) and p_{d_0} ($p_{z_0 \sin \theta}$) in Eq. (1) are $30 \mu\text{m}$ ($90 \mu\text{m}$) and 2.1 GeV (1.0 GeV), respectively.) We then evaluate the resolutions of primary vertices as a function of the number of tracks. The results are also shown in Fig. 1. As can be seen from this figure, our result is in good agreement with the ATLAS results [22]. Thus, in the following analysis, we use the above-mentioned procedure to determine the best-fit points of the decay vertices of pair-produced new particles.

3 Extending the Reach with DVs

Now, we discuss how and how well the reach for the new physics can be extended by using the information about the DVs. We are interested in the case where

- (a) the metastable particles are pair produced, and
- (b) the metastable particles decay into SM colored particles (*i.e.*, quarks and/or gluons) as well as possibly other particles.

In the pair production processes of new metastable particles, no hard particles are produced at the interaction point (assuming that the new particles decay after flying sizable amount of distance) except those from initial state radiation. For this reason, we do not try to determine the position of the interaction point in each event.^{#2} We instead

^{#2} We however note that the reconstruction of the primary vertex is possible if hard jets or leptons

use the distance between the two reconstructed DVs, $|\mathbf{r}_{\text{DV1}} - \mathbf{r}_{\text{DV2}}|$, as a discriminating variable in our study, where \mathbf{r}_{DV1} and \mathbf{r}_{DV2} are positions of the reconstructed vertices. As we demonstrate below, we may extend the LHC reach for new particles by combining conventional kinematical cuts with the new cuts based on $|\mathbf{r}_{\text{DV1}} - \mathbf{r}_{\text{DV2}}|$.

Although the strategy we propose is applicable to the class of models satisfying the conditions (a) and (b) mentioned above, a quantitative study needs to be performed on a model-by-model basis. Thus, we consider metastable gluino as an example, and discuss the implication of the study of the sub-millimeter DVs.

3.1 Gluino properties

Before discussing the LHC search for the metastable gluino with DVs, we summarize gluino properties which are important for the following discussion.

A gluino decays through the exchange of squarks. If squarks \tilde{q} are heavier than gluino \tilde{g} , and also if a neutralino $\tilde{\chi}^0$ and/or a chargino $\tilde{\chi}^\pm$ have a mass sufficiently smaller than the gluino mass, then the tree-level three-body decay processes $\tilde{g} \rightarrow \tilde{q}' q \tilde{\chi}^{0,\pm}$ dominate the two-body one $\tilde{g} \rightarrow \tilde{\chi}^0 g$, which occurs at one-loop level. The decay length of gluino strongly depends on the masses of the squarks exchanged in the tree-level three-body decay processes. Assuming that the first-generation squarks are sufficiently lighter than the second- and third-generation ones, the decay length of the gluino is approximately given by [11]

$$c\tau_{\tilde{g}} \simeq 200 \mu\text{m} \times \left(\frac{m_{\tilde{q}}}{10^3 \text{ TeV}} \right)^4 \left(\frac{2 \text{ TeV}}{m_{\tilde{g}}} \right)^5, \quad (2)$$

where $m_{\tilde{g}}$ is the gluino mass, $m_{\tilde{q}}$ is the masses of all the first-generation squarks (which are assume to be degenerate). In addition, the masses of bino and wino are assumed to be much smaller than the gluino mass, while the higgsino mass is assumed to be larger than the gluino mass. Note that the above expression should be multiplied by a factor of $\simeq 1/3$ if squarks in all generations are degenerate in mass. Eq. (2) indicates that the gluino decay length can be as long as $\gtrsim 100 \mu\text{m}$ for the PeV-scale squarks. Such heavy squarks, especially heavy stops, are in fact motivated by the measured value of the mass of the SM-like Higgs boson, $m_h \simeq 125 \text{ GeV}$ [32], as a large radiative correction from heavy stops can easily raise the Higgs-boson mass from its tree-level value [33], which is predicted to be smaller than the Z -boson mass [34] in the minimal supersymmetric SM (MSSM).

Even though the squark masses are at the PeV scale, gluino can still be around the TeV scale in a technically natural way since the gluino mass is protected by chiral symmetry. We may find a simple scenario for the mediation of SUSY-breaking to assure such a split mass spectrum [9, 10]. For example, if all of the SUSY-breaking fields in the hidden sector are charged under some symmetries, then the dimension-five operators that give rise to

are associated with the production point. It may also be possible to reconstruct the primary vertex using initial state radiation. Information about the primary vertex may also be utilized to eliminate the background.

the gaugino masses are forbidden. In this case, the gaugino masses are mainly induced by quantum effects, such as the anomaly mediation effects [35, 36] and threshold corrections at the SUSY-breaking scale [36, 37], and are suppressed by a loop factor compared with the gravitino mass $m_{3/2}$. The squark masses are, on the other hand, generated by dimension-six Kähler-type operators. If these operators are induced at the Planck scale, the squark masses are expected to be $\mathcal{O}(m_{3/2})$, while if they are induced at a lower scale, then the resultant squark masses become heavier. Motivated by this consideration, we regard the squark masses, and thus $c\tau_{\tilde{g}}$ as well through Eq. (2), as free parameters in the following analysis.

3.2 Gluino search with DVs

Now we discuss the gluino search with DVs. In this letter, in order to demonstrate that the LHC reach for gluino can be extended with the information about DVs, we impose a DV-based cut on top of the event selection criteria used in the ordinary gluino search. Because DV-based cut may significantly reduce the SM backgrounds, one had better optimize the cut parameters to maximize the reach for new physics. Such an issue is beyond the scope of this letter, and we leave it for future study [38].

In gluino searches, we focus on events with relatively high- p_T jets. In reconstructing DVs, this allows us to tighten the track selection cuts to $p_T > 1$ GeV in order to eliminate low- p_T tracks, whose impact-parameter resolutions are rather poor as can be seen from Eq. (1). (For tracks with $p_T > 1$ GeV, we found that the best-fit values of $\sigma_{d_0}(\infty)$ ($\sigma_{z_0 \sin \theta}(\infty)$) and p_{d_0} ($p_{z_0 \sin \theta}$) in Eq. (1) are 23 μm (78 μm) and 3.1 GeV (1.6 GeV), respectively.) We also require the tracks used for DV reconstruction to satisfy $|d_0| < 10$ mm and $|z_0| < 320$ mm [39].

For DV reconstruction, we only use tracks associated with four-highest p_T jets.^{#3} If one of these jets contains no track satisfying the above requirements, then we add the fifth-highest p_T jet. If more than one jets among these five high p_T jets do not offer any tracks which meet the above conditions, then we suppose that DV reconstruction is not possible in such an event. Since we do not know which pair of jets originate from a common parent gluino, we study all possible patterns of pairings out of the four jets. For each pairing, we find two DVs, each of which is reconstructed from tracks associated with the corresponding jet pair. Among the possible pairings, we adopt the one which minimizes an objective function that is defined by the sum of the weighted vertex χ^2 divided by the sum of the weights over the two DVs, where we use the same weight as that given in Ref. [29] (see Eq. (A.5) in Appendix for a concrete expression). We regard the vertices reconstructed for this jet pairing as the reconstructed DVs in the following analysis.

In order to see how the variable $|\mathbf{r}_{\text{DV1}} - \mathbf{r}_{\text{DV2}}|$ distributes, we perform MC simulation for the gluino pair production processes. We first fix the mass and the decay length $c\tau_{\tilde{g}}$ of gluino (as well as other MSSM parameters). Then, event samples for the gluino pair

^{#3}This reflects the event topology under consideration; gluinos are always pair-produced and each of them decays into two quarks and a neutralino.

production process are generated; `MadGraph5_aMC@NLO v2` [40] and `PYTHIA v8.2` are used for this purpose. We generate 50,000 events for each mass and lifetime of gluino. For each event, we determine the flight lengths of two gluinos using the lifetime of the gluino, and hence two decay vertices. The production point of each final-state particle is shifted by the flight length of its parent gluino. Signal event samples are normalized according to the NLL+NLO gluino pair production cross section [41]. The produced gluinos are forced to decay into first-generation quarks and a neutralino with a mass of 100 GeV; we refer to these samples as “light flavor samples.” After a fast detector simulation with `DELPHES v3` [42], we select only event samples in the signal region of `Meff-4j-2600` defined in the ATLAS gluino search [43], which adopts events with $E_T^{(\text{miss})} > 250$ GeV (with $E_T^{(\text{miss})}$ being the missing energy), $p_T(j_1) > 200$ GeV (with $p_T(j_i)$ being the transverse momentum of i -th jet), $p_T(j_4) > 150$ GeV, $\Delta\phi(j_{1,2,3,4}, E_T^{(\text{miss})})_{\text{min}} > 0.4$ (with $\Delta\phi$ being the azimuthal angle between the jet and the missing energy), aplanarity larger than 0.04, $E_T^{(\text{miss})}/m_{\text{eff}}(4) > 0.2$ (with $m_{\text{eff}}(4)$ being the scalar sum of $E_T^{(\text{miss})}$ and the transverse momenta of leading 4-jets), and $m_{\text{eff}}(\text{incl.}) > 2600$ GeV (with $m_{\text{eff}}(\text{incl.})$ being the scalar sum of $E_T^{(\text{miss})}$ and the transverse momenta of jets with $p_T > 50$ GeV).

In order to discuss the discovery reach, we should also consider backgrounds. As we have mentioned, we require the presence of DVs on top of the event selection conditions used in the ordinary gluino searches. The latter conditions drop most of the SM background, and thus most of the fake DV events are also expected to be eliminated. Since we impose relatively tight kinematical selection cuts (*i.e.*, `Meff-4j-2600`), we expect the properties of the SM background events relevant to tracking and DV reconstruction, such as the multiplicity and p_T of charged tracks, to resemble those of the signal events after applying the kinematical selection cuts. With this expectation, we approximate the background event samples which pass the kinematical selection cuts by the signal event samples with $c\tau_{\tilde{g}} = 0$. However, one possible difference between these two is that the SM background may contain b quarks while our signal event samples called “light flavor samples” only include the first-generation quarks. b quarks tend to be long-lived and thus may contribute to background considerably. To take into account this possibility, we generate event samples called “heavy flavor samples,” where the produced gluinos are forced to decay into b quarks, and use them as background samples to be conservative. We normalize the cross section of the background events to be 0.20 fb as observed in the ATLAS gluino search [43]. In addition, since we mainly consider DVs inside the beam pipe, we neglect background vertices from hadronic interactions in the detector materials and only consider background vertices which are mis-reconstructed as displaced ones due to the resolution of track impact parameters. With this simplification, we reject an event with a DV whose reconstructed position is inside the detector materials: *i.e.*, $22 \text{ mm} \leq |(\mathbf{r}_{\text{DV}})_T| \leq 25 \text{ mm}$, $29 \text{ mm} \leq |(\mathbf{r}_{\text{DV}})_T| \leq 38 \text{ mm}$, $46 \text{ mm} \leq |(\mathbf{r}_{\text{DV}})_T| \leq 73 \text{ mm}$, $84 \text{ mm} \leq |(\mathbf{r}_{\text{DV}})_T| \leq 111 \text{ mm}$, or $|(\mathbf{r}_{\text{DV}})_T| \geq 120 \text{ mm}$ [26, 44–46].

In Fig. 2a, we show the $|\mathbf{r}_{\text{DV}1} - \mathbf{r}_{\text{DV}2}|$ distribution in the signal region `Meff-4j-2600`. In addition, in Fig. 2b we plot the fraction of events passing the selection cut of $|\mathbf{r}_{\text{DV}1} - \mathbf{r}_{\text{DV}2}| > r_{\text{cut}}$ as a function of r_{cut} . Note that the background distribution deviates from

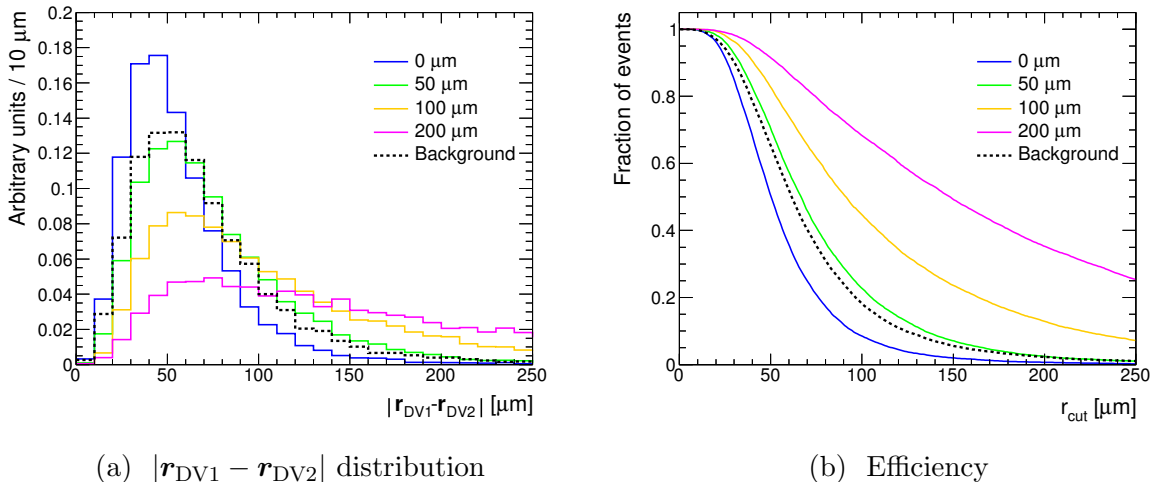


Figure 2: (a) $|r_{DV1} - r_{DV2}|$ distribution in the signal region **Meff-4j-2600** for various $c\tau_{\tilde{g}}$. (b) the fraction of events passing the selection cut of $|r_{DV1} - r_{DV2}| > r_{\text{cut}}$ as a function of r_{cut} . Here we set $m_{\tilde{g}} = 2.2$ TeV in both figures.

the signal distribution with $c\tau_{\tilde{g}} = 0$ because the background contains b hadrons in jets. These figures show that if we set r_{cut} to be $\gtrsim 100 \mu\text{m}$, then a significant fraction of SM background fails to pass the selection cut while a sizable number of signal events for $c\tau_{\tilde{g}} \gtrsim 100 \mu\text{m}$ remain after the cut. This observation indicates that this cut may be useful to probe a gluino with a decay length of $c\tau_{\tilde{g}} \gtrsim 100 \mu\text{m}$.

To demonstrate the performance of the new selection cut based on DVs, we show how far we can extend the discovery reach and exclusion limit of the gluino searches. We apply the cut to both signal and background events in the signal region **Meff-4j-2600** and estimate the expected exclusion and discovery reaches for gluino. We vary the cut parameter r_{cut} from $0 \mu\text{m}$ to $1000 \mu\text{m}$ by $20 \mu\text{m}$, and determine the highest value of the gluino mass as a gluino mass reach for each $c\tau_{\tilde{g}}$. For the integrated luminosity of $\mathcal{L} = 100 \text{ fb}^{-1}$ (1000 fb^{-1}) at the 13 TeV LHC, we find that $r_{\text{cut}} \sim 200 \mu\text{m}$ ($400 \mu\text{m}$) yields the best discovery and exclusion performance for a gluino with $c\tau_{\tilde{g}} \gtrsim 200 \mu\text{m}$.

For exclusion limits, we compute the expected 95% confidence level (CL) limits on the gluino mass using the CL_s prescription [48]. In Fig. 3, we show the expected limit on the gluino mass as a function of $c\tau_{\tilde{g}}$ based on the currently available luminosity of 13.3 fb^{-1} at the 13 TeV LHC. We can see that, even with the current data, the exclusion limit can be improved by about 80 and 120 GeV for $c\tau_{\tilde{g}} = 0.3$ and 1 mm, respectively. To compare the result with the current sensitivities of other gluino searches, we also show the 95% CL exclusion limits given by the ATLAS prompt-decay gluino search with the 13 TeV 13.3 fb^{-1} data (red dotted line) [43], the ATLAS DV search with the 8 TeV 20.3 fb^{-1} data (blue dot-dashed line) [2], and the ATLAS search of large ionization energy loss in the Pixel detector with the 13 TeV 3.2 fb^{-1} data (orange dotted line) [47]. The existing metastable gluino searches are insensitive to a gluino with $c\tau_{\tilde{g}} \lesssim 1$ mm, as shown in Fig. 3

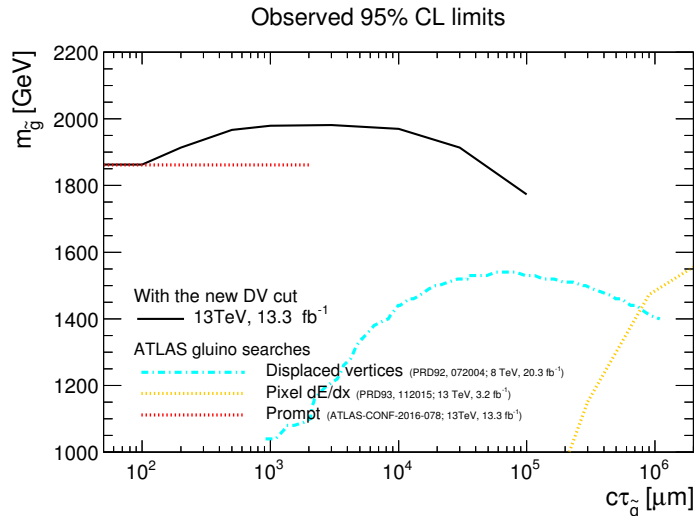


Figure 3: The 95% CL expected exclusion limits on the gluino mass with $\mathcal{L} = 13.3 \text{ fb}^{-1}$ at the 13 TeV LHC run as a function of $c\tau_{\tilde{g}}$ (black solid line). For comparison, we also show the 95% CL exclusion limits given by the ATLAS prompt-decay gluino search (red dotted line) [43], the ATLAS DV search (blue dot-dashed line) [2], and the ATLAS search of large ionization energy loss in the Pixel detector (orange dotted line) [47].

(blue dot-dashed and orange dotted lines), to which searches with the new DV cut may offer a good sensitivity. In this sense, this new search strategy plays a complementary role in probing metastable gluinos.

To see the future prospect, we also derive the expected 95% CL exclusion limits as well as 5σ discovery reach with larger luminosity. The expected discovery reach is determined by calculating the expected significance of discovery Z_0 [49]:

$$Z_0 = \sqrt{2 \{(S + B) \log(1 + S/B) - S\}}, \quad (3)$$

where S (B) is the expected number of signal (background) events. We then require Z_0 to be larger than 5 for discovery. In Fig. 4, we show the expected 95% CL exclusion limits and 5σ discovery reaches for gluino as functions of $c\tau_{\tilde{g}}$ for different values of integrated luminosity at the 13 TeV LHC run. Notice that the expected reaches for an extremely small $c\tau_{\tilde{g}}$ should correspond to those for the prompt-decay gluino with the same data set since the new DV cut plays no role in this case. As can be seen from this figure, the reach for the gluino can be extended with the help of the additional DV selection cut for $c\tau_{\tilde{g}} \gtrsim 100 \mu\text{m}$; for instance, for a gluino with $c\tau_{\tilde{g}} \sim \mathcal{O}(1\text{--}10) \text{ mm}$, the expected discovery reach for the gluino mass can be extended by as large as $\sim 300 \text{ GeV}$ (500 GeV) with an integrated luminosity of $\mathcal{L} = 100 \text{ fb}^{-1}$ (1000 fb^{-1}). Because charged tracks with $|d_0| > 10 \text{ mm}$ are not included in the analysis, and also because we reject all events with a DV whose reconstructed position radius is larger than 120 mm, the expected exclusion limits decrease for $c\tau_{\tilde{g}} \gtrsim 100 \text{ mm}$. Such a larger $c\tau_{\tilde{g}}$ region can however be covered by other long-lived gluino searches. (Remember that these numbers are based on the events in

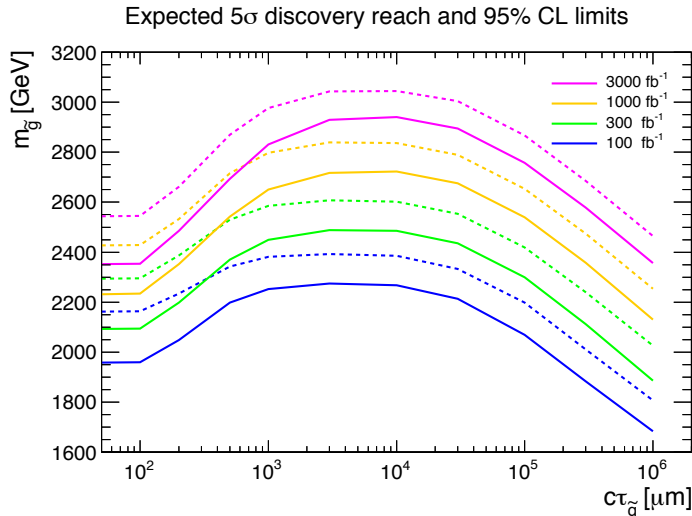


Figure 4: The expected 95% CL exclusion limits (dotted) and 5σ discovery reaches (solid) as functions of $c\tau_{\tilde{g}}$ for different values of integrated luminosity at the 13 TeV LHC run.

the signal region $M_{\text{eff}}-4j-2600$. For more accurate estimation of the improvement, one should carefully optimize the selection criteria, with which we may have better reach.)

3.3 Lifetime measurement

If a new metastable particle is discovered at the LHC, measurement of its lifetime is of crucial importance to understand the nature of new physics behind this metastable particle. In this subsection, we discuss the prospect of the lifetime measurement by means of the DV reconstruction method we have discussed.

To see the prospect of the lifetime measurement, we study the expected significance of rejection of a hypothesis that the gluino decay length is $c\tau_{\tilde{g}}^{(\text{hypo})}$ for gluino samples with a decay length of $c\tau_{\tilde{g}}$. Event samples are binned according to the DV distance $|\mathbf{r}_{\text{DV1}} - \mathbf{r}_{\text{DV2}}|$ of the events. Then the expected significance $\langle Z_{c\tau_{\tilde{g}}^{(\text{hypo})}} \rangle_{c\tau_{\tilde{g}}}$ is determined as

$\langle Z_{c\tau_{\tilde{g}}^{(\text{hypo})}} \rangle_{c\tau_{\tilde{g}}} \equiv \sqrt{\Delta\chi^2(c\tau_{\tilde{g}}^{(\text{hypo})}, c\tau_{\tilde{g}})}$, where

$$\Delta\chi^2(c\tau_{\tilde{g}}^{(\text{hypo})}, c\tau_{\tilde{g}}) = \sum_{\text{bin } i} \frac{\left\{ S_i(c\tau_{\tilde{g}}^{(\text{hypo})}) - S_i(c\tau_{\tilde{g}}) \right\}^2}{S_i(c\tau_{\tilde{g}}^{(\text{hypo})}) + B_i}. \quad (4)$$

Here, $S_i(c\tau)$ is the expected number of signal events in the bin i on the assumption that gluinos have a decay length of $c\tau$, while B_i is the number of SM background. We show the expected significance for $c\tau_{\tilde{g}}^{(\text{hypo})} = 0$ and $200 \mu\text{m}$ as a function of the gluino decay length $c\tau_{\tilde{g}}$ used to generate the data sample in Figs. 5a and 5b, respectively, for a gluino with a mass of 2.2 TeV. Here we use the visible cross-section $\epsilon\sigma$ of 8.8×10^{-2} fb for signal events, which is defined by the product of the production cross-section σ and

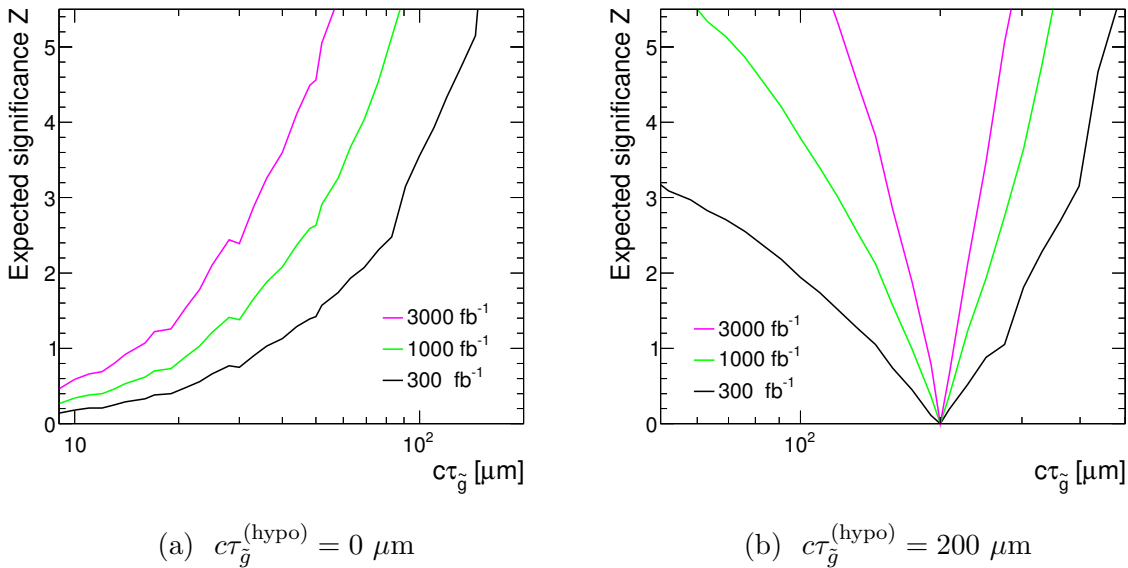


Figure 5: The expected significance of rejection $\langle Z_{c\tau_{\tilde{g}}^{(\text{hypo})}} \rangle_{c\tau_{\tilde{g}}}$ as a function of $c\tau_{\tilde{g}}$ for an integrated luminosity of 300, 1000, and 3000 fb^{-1} in the black, green, and purple lines, respectively. Here, we set $m_{\tilde{g}} = 2.2 \text{ TeV}$. See text for the definition of $\langle Z_{c\tau_{\tilde{g}}^{(\text{hypo})}} \rangle_{c\tau_{\tilde{g}}}$.

the fraction of signal events in the signal region **Meff-4j-2600** estimated from our fast detector simulation, ϵ . In Figs. 6a and 6b, we also show the expected upper and lower bounds on the decay length as a function of $c\tau_{\tilde{g}}$. From the figures, we find that a metastable gluino with $c\tau_{\tilde{g}} \gtrsim 25$ (50) μm can be distinguished from a promptly decaying one with the significance of 2σ (5σ) with an integrated luminosity of 3000 fb^{-1} . Moreover, Fig. 5b shows that the decay length of a gluino with $c\tau_{\tilde{g}} \sim \mathcal{O}(100)$ μm can be measured with an $\mathcal{O}(1)$ accuracy at the high-luminosity LHC. With such a measurement, we may probe the squark mass scale $m_{\tilde{q}}$ via Eq. (2) even though squarks are inaccessible at the LHC, which sheds light on the SUSY mass spectrum as well as the mediation mechanism of SUSY-breaking effects.

4 Conclusions and Discussion

In this letter, we have discussed a method of reconstructing DVs that originate from decay of metastable particles on the assumption that these metastable particles are always pair-produced and their decay products contain high- p_T jets. We especially consider gluinos in the SUSY models as an example, which tend to be metastable when squarks have masses much larger than the TeV scale. It is found that this method can separate out DVs if the gluino decay length is $\gtrsim 100$ μm . Then, we have seen that an event selection cut based on this DV reconstruction may be utilized to improve the potential of the gluino searches for a gluino with $c\tau_{\tilde{g}} \gtrsim 100$ μm . In particular, if $c\tau_{\tilde{g}} \sim \mathcal{O}(1-10)$ mm, then the

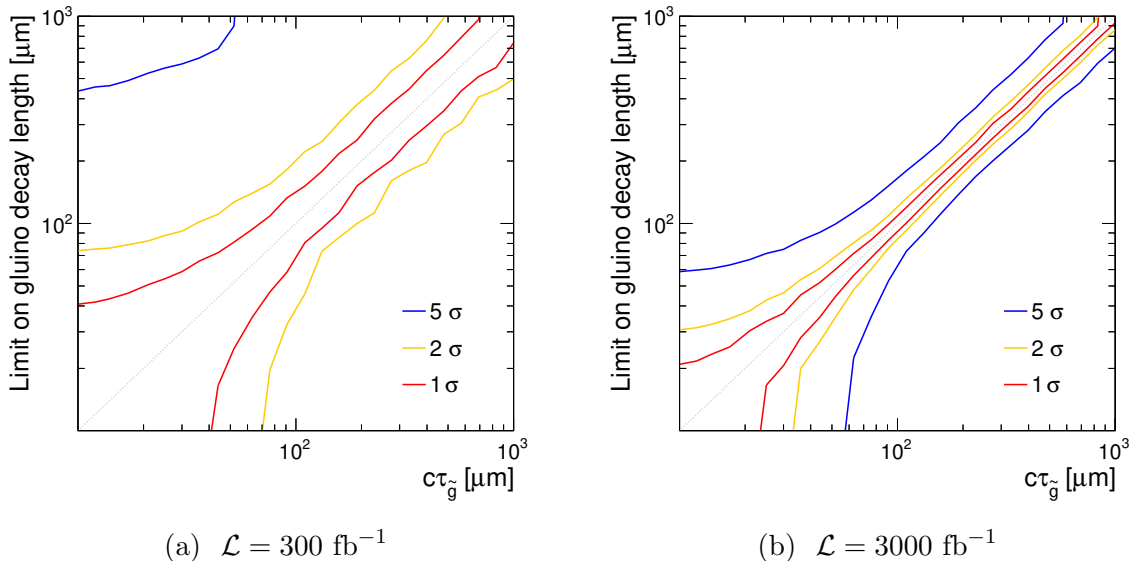


Figure 6: The expected upper and lower bounds decay length of gluino as a function of the underlying value of $c\tau_{\tilde{g}}$. Here, we set $m_{\tilde{g}} = 2.2 \text{ TeV}$.

exclusion and discovery reaches for the gluino mass can be extended by about 370 GeV and 500 GeV, respectively, with an integrated luminosity of 1000 fb^{-1} at the 13 TeV LHC. Furthermore, with an integrated luminosity of 3000 fb^{-1} , it is possible to measure the gluino decay length with an $\mathcal{O}(1)$ accuracy for a gluino with $c\tau_{\tilde{g}} \sim \mathcal{O}(100) \mu\text{m}$ and $m_{\tilde{g}} = 2.2 \text{ TeV}$, which may allow us to probe the PeV-scale squarks indirectly. Although we have concentrated on metastable gluinos in SUSY models, a similar technique may be used to probe DV signatures from other metastable particles. A more extensive study will be done elsewhere [38].

Acknowledgments

The authors thank T. Yamanaka and S. Adachi for useful discussion. This work was supported by the Grant-in-Aid for Scientific Research on Scientific Research C (No.26400239 [TM]), Young Scientists B (No.15K17653 [HO]), and Innovative Areas (No.16H06489 [OJ], No.16H06490 [TM]).

Appendix: Vertexing Method

Here, we give a brief review on the vertexing method exploited in our analysis, as well as a concrete expression for the objective function used to determine the reconstructed DVs.

Our vertexing method is based on the adaptive vertex fitting algorithm [29]. In this algorithm, an initial vertex position is found using the FSMW method [30] for a pair of

jets in question. This method first defines a crossing point for a pair of the two tracks chosen from each jet as the closest midpoint of these tracks. We then assign a weight to this crossing point,

$$w \equiv (d + d_{\min})^{-\frac{1}{2}} , \quad (\text{A.1})$$

where d is the distance between the two tracks, and we set $d_{\min} = 10 \mu\text{m}$ following Ref. [29]. This weight gets larger if the distance between the two tracks associated with the crossing point is smaller. Next, for a spatial coordinate, say, the x -coordinate, we consider a distribution of the crossing points and define a weighted interval for the distribution as the length of the interval divided by the sum of the weights of the points in the interval. We then find the smallest weighted interval that covers at least 40% of all the points. This process is recursively performed for the obtained smallest weighted interval until the interval contains only two points, and eventually the midpoint of the remaining two points is defined as the x -coordinate of the initial vertex position. We perform this procedure for each spatial direction.

For the vertex position \mathbf{v} determined above, we define

$$\chi_i^2(\mathbf{v}) \equiv \frac{d_i^2(\mathbf{v})}{\sigma_{d_0}^2 + \sigma_{z_0 \sin \theta}^2} , \quad (\text{A.2})$$

for each track i , where $d_i(\mathbf{v})$ denotes its distance from the vertex \mathbf{v} . We further assign a weight w_i to each track that is defined by

$$w_i(\chi_i^2) \equiv \frac{\exp(-\chi_i^2/2T)}{\exp(-\chi_i^2/2T) + \exp(-\chi_c^2/2T)} , \quad (\text{A.3})$$

where we use $\chi_c = 3$ [29] and T is a parameter that we choose in the following. As can be seen from this expression, if a track is far away from the vertex \mathbf{v} , a fairly small weight is assigned to the track. Then, we determine a new vertex position by solving

$$\sum_i w_i(\chi_i^2(\mathbf{v})) \chi_i(\mathbf{v}_{\text{new}}) \frac{\partial \chi_i(\mathbf{v}_{\text{new}})}{\partial \mathbf{v}} = 0 , \quad (\text{A.4})$$

with respect to \mathbf{v}_{new} . This new vertex position (\mathbf{v}_{new}) is then used as an initial vertex position to repeat this process. We iterate the above process with varying the parameter T as $T = 256 \rightarrow 64 \rightarrow 16 \rightarrow 4 \rightarrow 1 \rightarrow 1 \rightarrow \dots$ until $T = 1$ and the vertex position converges within $1 \mu\text{m}$.

As mentioned in Sec. 3.2, the weight w_i defined in Eq. (A.3) is also used to determine the jet pairing for the reconstruction of DVs out of four jets. Among the three possible pairings of the four jets, we choose the one which minimizes

$$\chi^2 \equiv \frac{\sum_{i \in \text{trk}(\mathbf{v}_1)} w_i(\chi_i^2(\mathbf{v}_1)) \chi_i^2(\mathbf{v}_1) + \sum_{j \in \text{trk}(\mathbf{v}_2)} w_j(\chi_j^2(\mathbf{v}_2)) \chi_j^2(\mathbf{v}_2)}{\sum_{i \in \text{trk}(\mathbf{v}_1)} w_i(\chi_i^2(\mathbf{v}_1)) + \sum_{j \in \text{trk}(\mathbf{v}_2)} w_j(\chi_j^2(\mathbf{v}_2))} , \quad (\text{A.5})$$

where $\text{trk}(\mathbf{v}_{1,2})$ denotes the set of tracks associated with the DV $\mathbf{v}_{1,2}$ reconstructed for each pair of jets, and we take $T = 1$ and $\chi_c = 3$ in the weights. We define the reconstructed DVs by $\mathbf{r}_{\text{DV}1,2} \equiv \mathbf{v}_{1,2}$ for the jet pairing that minimizes this χ^2 , and use them in our analysis.

References

- [1] M. Fairbairn, A. C. Kraan, D. A. Milstead, T. Sjostrand, P. Z. Skands, and T. Sloan, Phys. Rept. **438**, 1 (2007), arXiv:hep-ph/0611040 [hep-ph].
- [2] G. Aad *et al.* (ATLAS), Phys. Rev. **D92**, 072004 (2015), arXiv:1504.05162 [hep-ex].
- [3] G. Aad *et al.* (ATLAS), Phys. Rev. **D88**, 112006 (2013), arXiv:1310.3675 [hep-ex].
- [4] J. L. Feng, T. Moroi, L. Randall, M. Strassler, and S.-f. Su, Phys. Rev. Lett. **83**, 1731 (1999), arXiv:hep-ph/9904250 [hep-ph].
- [5] M. Ibe, T. Moroi, and T. T. Yanagida, Phys. Lett. **B644**, 355 (2007), arXiv:hep-ph/0610277 [hep-ph].
- [6] S. Asai, T. Moroi, K. Nishihara, and T. T. Yanagida, Phys. Lett. **B653**, 81 (2007), arXiv:0705.3086 [hep-ph]; S. Asai, T. Moroi, and T. T. Yanagida, Phys. Lett. **B664**, 185 (2008), arXiv:0802.3725 [hep-ph]; S. Asai, Y. Azuma, O. Jinnouchi, T. Moroi, S. Shirai, and T. T. Yanagida, Phys. Lett. **B672**, 339 (2009), arXiv:0807.4987 [hep-ph].
- [7] N. Nagata, H. Otono, and S. Shirai, (2017), arXiv:1701.07664 [hep-ph].
- [8] V. Khachatryan *et al.* (CMS), Phys. Rev. D (2016), 10.1103/PhysRevD.95.012009, [Phys. Rev.D95,012009(2017)], arXiv:1610.05133 [hep-ex].
- [9] J. D. Wells, (2003), arXiv:hep-ph/0306127 [hep-ph]; N. Arkani-Hamed and S. Dimopoulos, JHEP **0506**, 073 (2005), arXiv:hep-th/0405159 [hep-th]; G. Giudice and A. Romanino, Nucl.Phys. **B699**, 65 (2004), arXiv:hep-ph/0406088 [hep-ph]; N. Arkani-Hamed, S. Dimopoulos, G. Giudice, and A. Romanino, Nucl.Phys. **B709**, 3 (2005), arXiv:hep-ph/0409232 [hep-ph]; J. D. Wells, Phys.Rev. **D71**, 015013 (2005), arXiv:hep-ph/0411041 [hep-ph].
- [10] L. J. Hall and Y. Nomura, JHEP **1201**, 082 (2012), arXiv:1111.4519 [hep-ph]; L. J. Hall, Y. Nomura, and S. Shirai, JHEP **1301**, 036 (2013), arXiv:1210.2395 [hep-ph]; M. Ibe and T. T. Yanagida, Phys.Lett. **B709**, 374 (2012), arXiv:1112.2462 [hep-ph]; M. Ibe, S. Matsumoto, and T. T. Yanagida, Phys.Rev. **D85**, 095011 (2012), arXiv:1202.2253 [hep-ph]; A. Arvanitaki, N. Craig, S. Dimopoulos, and G. Villadoro, JHEP **1302**, 126 (2013), arXiv:1210.0555 [hep-ph]; N. Arkani-Hamed, A. Gupta, D. E. Kaplan, N. Weiner, and T. Zorawski, (2012), arXiv:1212.6971 [hep-ph]; J. L. Evans, M. Ibe, K. A. Olive, and T. T. Yanagida, Eur.Phys.J. **C73**, 2468 (2013), arXiv:1302.5346 [hep-ph]; J. L. Evans, K. A. Olive, M. Ibe, and T. T. Yanagida, Eur.Phys.J. **C73**, 2611 (2013), arXiv:1305.7461 [hep-ph].
- [11] M. Toharia and J. D. Wells, JHEP **02**, 015 (2006), arXiv:hep-ph/0503175 [hep-ph]; P. Gambino, G. F. Giudice, and P. Slavich, Nucl. Phys. **B726**, 35 (2005), arXiv:hep-ph/0506214 [hep-ph]; R. Sato, S. Shirai, and K. Tobioka, JHEP **11**, 041 (2012), arXiv:1207.3608 [hep-ph].
- [12] G. F. Giudice and R. Rattazzi, Phys. Rept. **322**, 419 (1999), arXiv:hep-ph/9801271 [hep-ph].

- [13] P. Draper, P. Meade, M. Reece, and D. Shih, Phys. Rev. **D85**, 095007 (2012), arXiv:1112.3068 [hep-ph]; J. A. Evans and J. Shelton, JHEP **04**, 056 (2016), arXiv:1601.01326 [hep-ph].
- [14] R. Barbier *et al.*, Phys. Rept. **420**, 1 (2005), arXiv:hep-ph/0406039 [hep-ph].
- [15] P. W. Graham, D. E. Kaplan, S. Rajendran, and P. Saraswat, JHEP **07**, 149 (2012), arXiv:1204.6038 [hep-ph]; K. Barry, P. W. Graham, and S. Rajendran, Phys. Rev. **D89**, 054003 (2014), arXiv:1310.3853 [hep-ph]; C. Csaki, E. Kuflik, and T. Volansky, Phys. Rev. Lett. **112**, 131801 (2014), arXiv:1309.5957 [hep-ph]; C. Csaki, E. Kuflik, S. Lombardo, O. Slone, and T. Volansky, JHEP **08**, 016 (2015), arXiv:1505.00784 [hep-ph].
- [16] Z. Chacko, H.-S. Goh, and R. Harnik, Phys. Rev. Lett. **96**, 231802 (2006), arXiv:hep-ph/0506256 [hep-ph]; G. Burdman, Z. Chacko, H.-S. Goh, and R. Harnik, JHEP **02**, 009 (2007), arXiv:hep-ph/0609152 [hep-ph]; H. Cai, H.-C. Cheng, and J. Terning, JHEP **05**, 045 (2009), arXiv:0812.0843 [hep-ph].
- [17] Z. Chacko, D. Curtin, and C. B. Verhaaren, Phys. Rev. **D94**, 011504 (2016), arXiv:1512.05782 [hep-ph].
- [18] M. J. Strassler and K. M. Zurek, Phys. Lett. **B651**, 374 (2007), arXiv:hep-ph/0604261 [hep-ph].
- [19] J. Barnard, P. Cox, T. Gherghetta, and A. Spray, JHEP **03**, 003 (2016), arXiv:1510.06405 [hep-ph].
- [20] S. Chang and M. A. Luty, (2009), arXiv:0906.5013 [hep-ph]; R. T. Co, F. D’Eramo, L. J. Hall, and D. Pappadopulo, JCAP **1512**, 024 (2015), arXiv:1506.07532 [hep-ph].
- [21] L. Basso, A. Belyaev, S. Moretti, and C. H. Shepherd-Themistocleous, Phys. Rev. **D80**, 055030 (2009), arXiv:0812.4313 [hep-ph]; J. C. Helo, M. Hirsch, and S. Kovalenko, Phys. Rev. **D89**, 073005 (2014), [Erratum: Phys. Rev.D93,no.9,099902(2016)], arXiv:1312.2900 [hep-ph]; E. Izaguirre and B. Shuve, Phys. Rev. **D91**, 093010 (2015), arXiv:1504.02470 [hep-ph].
- [22] *Vertex Reconstruction Performance of the ATLAS Detector at $\sqrt{s} = 13$ TeV*, Tech. Rep. ATL-PHYS-PUB-2015-026 (CERN, Geneva, 2015).
- [23] *Performance of primary vertex reconstruction in proton-proton collisions at $\sqrt{s} = 7$ TeV in the ATLAS experiment*, Tech. Rep. ATLAS-CONF-2010-069 (CERN, Geneva, 2010); M. Aaboud *et al.* (ATLAS), (2016), arXiv:1611.10235 [physics.ins-det].
- [24] S. Chatrchyan *et al.* (CMS), JINST **9**, P10009 (2014), arXiv:1405.6569 [physics.ins-det]; CMS (CMS Collaboration), *Primary vertex resolution in 2016*, Tech. Rep. CMS-DP-2016-041 (2016).
- [25] ATLAS, “*Impact Parameter Resolution*,” <https://atlas.web.cern.ch/Atlas/GROUPS/PHYSICS/PLOTS/IDTR-2015-007/> (2015); *Track Reconstruction Performance of the ATLAS Inner Detector at $\sqrt{s} = 13$ TeV*, Tech. Rep. ATL-PHYS-PUB-2015-018 (CERN, Geneva, 2015).

- [26] M. Capeans, G. Darbo, K. Einsweiler, M. Elsing, T. Flick, M. Garcia-Sciveres, C. Gemme, H. Pernegger, O. Rohne, and R. Vuillermet, *ATLAS Insertable B-Layer Technical Design Report*, Tech. Rep. CERN-LHCC-2010-013. ATLAS-TDR-19 (2010).
- [27] G. Aad *et al.* (ATLAS), (2009), arXiv:0901.0512 [hep-ex].
- [28] ATLAS, “*Impact Parameter Resolution Using 2016 MB Data*,” <https://atlas.web.cern.ch/Atlas/GROUPS/PHYSICS/PLOTS/IDTR-2016-018/> (2016).
- [29] R. Fruhwirth, W. Waltenberger, and P. Vanlaer, *J. Phys.* **G34**, N343 (2007).
- [30] D. R. Bickel and R. Fruhwirth, *Computational Statistics & Data Analysis* **50**, 3500 (2006), arXiv:math/0505419 [math].
- [31] T. Sjostrand, S. Mrenna, and P. Z. Skands, *Comput. Phys. Commun.* **178**, 852 (2008), arXiv:0710.3820 [hep-ph].
- [32] G. Aad *et al.* (ATLAS, CMS), *Phys. Rev. Lett.* **114**, 191803 (2015), arXiv:1503.07589 [hep-ex].
- [33] Y. Okada, M. Yamaguchi, and T. Yanagida, *Prog.Theor.Phys.* **85**, 1 (1991); Y. Okada, M. Yamaguchi, and T. Yanagida, *Phys.Lett.* **B262**, 54 (1991); J. R. Ellis, G. Ridolfi, and F. Zwirner, *Phys.Lett.* **B257**, 83 (1991); H. E. Haber and R. Hempfling, *Phys.Rev.Lett.* **66**, 1815 (1991); J. R. Ellis, G. Ridolfi, and F. Zwirner, *Phys.Lett.* **B262**, 477 (1991).
- [34] K. Inoue, A. Kakuto, H. Komatsu, and S. Takeshita, *Prog.Theor.Phys.* **67**, 1889 (1982); R. A. Flores and M. Sher, *Annals Phys.* **148**, 95 (1983).
- [35] L. Randall and R. Sundrum, *Nucl. Phys.* **B557**, 79 (1999), arXiv:hep-th/9810155 [hep-th].
- [36] G. F. Giudice, M. A. Luty, H. Murayama, and R. Rattazzi, *JHEP* **12**, 027 (1998), arXiv:hep-ph/9810442 [hep-ph].
- [37] D. M. Pierce, J. A. Bagger, K. T. Matchev, and R.-j. Zhang, *Nucl. Phys.* **B491**, 3 (1997), arXiv:hep-ph/9606211 [hep-ph].
- [38] H. Ito, O. Jinnouchi, T. Moroi, N. Nagata, and H. Otono, work in progress.
- [39] G. Aad *et al.* (ATLAS), *Phys. Rev.* **D92**, 012010 (2015), arXiv:1504.03634 [hep-ex].
- [40] J. Alwall, R. Frederix, S. Frixione, V. Hirschi, F. Maltoni, O. Mattelaer, H. S. Shao, T. Stelzer, P. Torrielli, and M. Zaro, *JHEP* **07**, 079 (2014), arXiv:1405.0301 [hep-ph].
- [41] C. Borschensky, M. Krämer, A. Kulesza, M. Mangano, S. Padhi, T. Plehn, and X. Portell, *Eur. Phys. J.* **C74**, 3174 (2014), arXiv:1407.5066 [hep-ph].
- [42] J. de Favereau *et al.* (DELPHES 3), *JHEP* **1402**, 057 (2014), arXiv:1307.6346 [hep-ex].
- [43] *Further searches for squarks and gluinos in final states with jets and missing transverse momentum at $\sqrt{s} = 13$ TeV with the ATLAS detector*, Tech. Rep. ATLAS-CONF-2016-078 (CERN, Geneva, 2016).

- [44] ATLAS Collaboration, JINST **3**, S08003 (2008).
- [45] A. Miucci, Journal of Instrumentation **9**, C02018 (2014).
- [46] G. A. M. Aaboud *et al.*, Journal of Instrumentation **11**, P11020 (2016).
- [47] M. Aaboud *et al.* (ATLAS), Phys. Rev. **D93**, 112015 (2016), arXiv:1604.04520 [hep-ex].
- [48] A. L. Read, *Advanced Statistical Techniques in Particle Physics. Proceedings, Conference, Durham, UK, March 18-22, 2002*, J. Phys. **G28**, 2693 (2002); T. Junk, Nucl. Instrum. Meth. **A434**, 435 (1999), arXiv:hep-ex/9902006 [hep-ex].
- [49] G. Cowan, K. Cranmer, E. Gross, and O. Vitells, Eur. Phys. J. **C71**, 1554 (2011), [Erratum: Eur. Phys. J. **C73**, 2501 (2013)], arXiv:1007.1727 [physics.data-an].